NJC

Accepted Manuscript

This is an *Accepted Manuscript*, which has been through the Royal Society of Chemistry peer review process and has been accepted for publication.

Accepted Manuscripts are published online shortly after acceptance, before technical editing, formatting and proof reading. Using this free service, authors can make their results available to the community, in citable form, before we publish the edited article. We will replace this *Accepted Manuscript* with the edited and formatted *Advance Article* as soon as it is available.

You can find more information about *Accepted Manuscripts* in the Information for Authors.

Please note that technical editing may introduce minor changes to the text and/or graphics, which may alter content. The journal's standard Terms & Conditions and the Ethical guidelines still apply. In no event shall the Royal Society of Chemistry be held responsible for any errors or omissions in this *Accepted Manuscript* or any consequences arising from the use of any information it contains.

ROYAL SOCIETY OF CHEMISTRY

www.rsc.org/njc

Highly efficient removal of TiO_2 nanoparticles from aquatic bodies by silica microspheres impregnated Ca-alginate

Hirakendu Basu, Mehzabin Vivek Pimple, Rakesh Kumar Singhal

Analytical Chemistry Division
Bhabha Atomic Research Centre, Trombay, Mumbai -400085, India
E mail: rsinghal@barc.gov.in ;Tel:91-22-25592233 fax No 91-22-25505151

Abstract

A novel material "calcium–alginate–silica microsphere" (Cal-Alg-SM) bead was developed by impregnating silica microsphere in calcium alginate. These beads were highly efficient in the removal of TiO_2 nanoparticles from aquatic bodies without disturbing its physicochemical characteristics. The optimum composition of the beads was 10% loading of silica microspheres into 4% Ca-alginate matrix. They were formed by controlled addition of homogenised mixture of SM and Na-alginate solution into 0.4M $CaCl_2$ solution. Cal-Alg-SM beads were characterized by measuring zeta potential, taking Fourier Transform Infra Red spectra and Scanning Electron Microscope hyphenated with Energy dispersive spectrometer mapping both before and after the uptake. Uptake studies carried out in batch mode, showed that Cal-Alg-SM beads are very effective for removal of TiO_2 nanoparticles in the pH range of 3-5 and the sorption was more than 90% in the concentration range of 10–500 µg mL^{-1}. Beads were successfully tested with lake and groundwater samples spiked with TiO_2 nanoparticles. Sorption isotherm was seen to follow Langmuir model and the uptake capacity evaluated was 29.9 mg g^{-1}. Mechanism of sorption was proposed based on the zeta potential values of the SM and TiO_2 nanopartices at different pH.

***Keywords*:** Silica microsphere, Titanium oxide, Calcium alginate, Sorption isotherm, Nano particle.

1.0 **Introduction**

With the growth of industry and development of nanotechnology, there has been a tremendous growth in the application of nanoparticles (NPs) for various uses like antibacterial materials, drug delivery systems, cosmetics, sunscreens and electronics.[1-4] NPs are defined as objects with at least one of its three dimensions in the range of 1–100 nm.[5-6] The smaller size of NPs ensures a large surface area per unit mass. Compared to fine particles, NPs of the same composition generally possess dramatically different physicochemical properties. Since surface properties, such as energy level, electronic structure, and reactivity are quite different from bulk, the bioactivity of NPs will be different from that of the bulk analogue.[7-8]

Traditionally, TiO_2 is considered as poorly soluble, low toxicity particles[9-10] and TiO_2 nanoparticles (TiO_2 NP) have been widely used in industrial and consumer products due to their stronger catalytic activity when compared to bulk TiO_2. TiO_2 NP is a white pigment. Because of its brightness and very high refractive index it is widely used.[11-13] TiO_2 NP are used in the industries like paints, pharmaceuticals, coatings, food products, cosmetics, plastics, papers, inks, toothpaste etc.[14-16] In recent times, concerns have been raised that these same properties of TiO_2 NP may throw challenges to human health because of its unique bioactivity.[17-18] Many in vitro and in vivo toxicological studies showed adverse effect of TiO_2 NPs on living organisms.[19-20] Different animal models employing multiple exposure routes of administration, including inhalation, oral intake, dermal exposure, intravenous injection etc. have been intensively used in these studies.[21-22] Studies have also revealed that TiO_2 NPs are more toxic than bulk.[23-24] TiO_2 has been classified as a Group 2B carcinogen by the International Agency for Research on Cancer (IARC).[25] Wide applications of TiO_2 NPs pose potential for environmental release which inevitably allows for a potential health risk to the eco-system and to the humans.[26]

Removal of pollutants from aquatic medium using adsorption phenomenon is a common practice, in which the pollutants are accumulated on any solid surface. Various adsorbents have been developed over the years and used for water treatment using different processes[27-31] but isolation of nanoparticles from aquatic stream is still a challenging task. Nano-filtration or ultra-filtration can be useful, but they are not cost effective and practical field application for a large quantity of water may not be physically viable. A large number of studies have been carried out by using silica microspheres[32-34] for removal of various pollutants from aquatic environments including dyes heavy metals and radionuclides[35-38]. They are very effective in removal as they have large surface area, well-defined and adjustable pore structure, narrow distribution of the pore size.[39-40] These spheres can be obtained by the synthesis of core–shell type particles. These core–shell particles often exhibit properties that are substantially different from those of the template core because of higher surface area, different surface chemical compositions, increased stability and different optical and magnetic properties.[41-43] Such particles can be applied in various fields including catalysis, coatings, capsule agents for drug delivery, composite materials.[44-47]

Methods of fabrication of hollow or micro silica spheres mostly involve removing the core by dissolution into solvents or by calcinations. This can be achieved in two different steps, i.e., formation of composite particle, followed by removal of inner structure leaving behind the core with hollow space. It is also possible to synthesize the silica microsphere in one-step process, which meant that the formation of the inorganic shells and the dissolution of core particles occurred in the same medium.[48-50]

Although silica microspheres (SM) can be selective towards TiO_2 NP, sufficiently high sorption capacity could be achieved by high specific surface areas i.e. smaller size and hollow or

porous nature of the microspheres. But separation of the powdered sorbent from the water sample becomes an issue. In addition to this there is definite probability of leaching of its constituents into water[51-52], therefore it is always advisable to immobilise the sorbent in the second medium.[53-56] The use of alginate as an immobilizing agent in most applications rests in its ability to form heat-stable strong gels which can be developed at room temperatures and are quiet stable.[57-60]

This present study was devoted to the synthesis and characterisation of silica microsphere impregnated calcium alginate beads (Cal-Alg-SM) and thereby removal of TiO_2 NP from the natural water. These beads can be used in the pH range of 3.0–5.0 and can reduce TiO_2 NP concentration as low as 10 ng mL^{-1}. The quality of water was monitored at various stages of the experiments. The sorption capacity of the beads was evaluated and verified by fitting in isotherm model (Langmuir). Influences of pH, contact time on sorption and kinetics were also tested.

2.0 Experimental

2.1 Chemical and reagent

All the reagents used in this work were obtained from Sigma Aldrich. The analytical grade chemicals were used without any pre-treatment. Demineralised water having resistivity 0.01 cm^{-1} and DOC (Dissolved Organic Carbon) <5 ng mL^{-1} was used throughout the experiment.

2.2 Sample preparation

Water samples were contaminated with TiO_2 NP powder procured from Nanoshel having stock no. NS6130-03-350. TiO_2 NP was characterised by XRD, Raman Spectroscopy and DLS prior to its use. Working TiO_2 NP suspensions in the range of 10 – 10000 µg mL^{-1} were prepared by accurately weighing the TiO_2 NP powder and mixing it in water followed by ultrasonication (Retsch UR1, 35 kHz) for 6h. Lake & groundwater samples used for the study were collected

from Trombay region, Mumbai, India having latitude 19°00'498 (N) and longitude 72°55'136. Samples were collected in one litre polypropylene bottles and filtered through 0.45µm filter paper attached to suction filtration assembly (Millipore) before use. Different physicochemical properties were measured before and after contamination.

2.3 Synthesis of silica microspheres

Synthesis of SM involves two steps. In the first step, monodispersed polystyrene (PS) particles were prepared by emulsion polymerization. Measured quantity of styrene (10g), polyvinylpyrrolidone (PVP) (1.5g) and water (90mL) were charged into a teflon lined SS autoclave. The solution was stirred and deoxygenated by passing N_2 at room temperature for 30 min. The mixture was then slowly heated to 70 ºC, followed by addition of aqueous solution containing potassium peroxodisulfate and the reaction was continued at 70 ºC for 24 h in the autoclave.[33,36] In the second step, the PVP functionalized PS latexes were reacted with tetraethyl orthosilicate (TEOS) in a solution of ammonia in ethanol to yield silica coated latex particles in a seeded growth process. In a typical procedure, PS emulsion (50mL) and NH_4OH (4mL) were added into ethanol (40mL) under stirring and the mixture was kept at 30 ºC. Then, TEOS was added slowly to the suspension under stirring at 30 ºC at a rate of 1 mLh^{-1} using a peristaltic pump and the reaction mixture was stirred for an additional 5 h. The suspended particles were separated using ultracentrifuge (Ultra 5.0, Hanil Scientific) at 35000 rpm for 2 h. Then the dried particles were treated with toluene to dissolve the PS and to make it porous and hollow and again washed and dried before use.[33,36]

2.4 Preparation of silica microspheres (SM) impregnated calcium alginate (Cal-Alg-SM) beads

In order to ease the separation of SM from the aquatic medium the SM was impregnated in alginate matrix. A 0.4 M solution of sodium alginate (Na-Alginate) in 100 mL of water was prepared. Weighed SM [10% (wt./vol.)] was mixed thoroughly in the solution to make it homogeneous. Then the mixture was stirred (600 rpm) for 5 h taken in polypropylene bottles and was added drop wise into 250 mL 4% calcium chloride ($CaCl_2$) solution using a peristaltic pump. Na alginate reacted with $CaCl_2$ to form beads of Ca alginate, entrapping the SM within it. The beads were stable, homogenous and permeable to water.

2.5 Characterisation

The zeta potential and size distribution of SM and TiO_2 NP suspensions were measured using laser based dynamic light scattering (Melvern: Zeta sizer nano ZS). Zeta potential was recorded at different pH values using an auto titrator attached to the zeta sizer. The morphology of the sorbent was characterised by using Scanning Electron Microscope coupled with Energy Dispersive X-ray Spectrometry (SEM-EDS) (Instrument Model No. VEGA MV 2300T). ATR-FTIR spectra of the sorbent at various stages were collected in the wavelength range of 500–4000 cm^{-1} with a spectrum resolution of 4 cm^{-1}using Attenuated Total Reflectance Fourier Transform Infra Red spectrometer equipped with the universal ATR as an internal reflection accessory having composite zinc selenide (ZnSe) optics and diamond crystal (ATRFTIR; Make Bruker, Model ALPHA-P).

2.6 Sorption experiment

The sorption studies of TiO_2 NP on Cal-Alg-SM beads were carried out in batch process. Measured quantity of TiO_2 NP suspension of desired concentration was taken into a polypropylene bottle and known weight of sorbent was added into it and shaken intermittently for 24 h to attain the equilibrium. Beads were then separated by decantation. The TiO_2 NP

concentrations were determined in remaining and the amount of TiO_2 NP sorbed was calculated from following equation (Eq-1),

$$Q_e = \frac{(C_o - C_e) \times V}{W} \quad (1)$$

where Q_e is the sorption capacity (mg g^{-1}) at equilibrium, C_o and C_e are the initial and equilibrium TiO_2 NP concentrations (mg L^{-1}) respectively; V is the volume (mL) of solution and W is the mass (g) of sorbent used. Relative standard deviations were found to be within ± 2.0%.

The effect of contact time (1 min to 30 h) was examined with initial TiO_2 NP concentrations of 100 mg L^{-1}. The effect of equilibrium pH was were investigated by adjusting the pH from 1 to 10 using 0.1 M HNO_3 and 0.1 M NaOH under an initial TiO_2 NP concentration of 100 mg L^{-1}.

2.7 Measurement of physicochemical characteristics & concentration of major and trace metal ions

Various physicochemical characteristics like pH, conductivity and redox potential were measured by using pH meter and conductivity meter (Model PICO$^+$, Lab India). The concentrations of various metal ions were either measured by Atomic Absorption Spectrometry (AAS), Inductive Coupled Plasma-Optical Emission Spectroscopy (ICP-OES) or Dionex Ion Chromatrography [Reagent Free Ion Chromatography System (RFICS) 2000]. The calibrations for all the elements were carried out by using ICP grade standards in HNO_3 medium.

2.8 Determination of TiO_2 NP concentration

Concentration of TiO_2 NP was determined in terms of total elemental concentration of titanium and was converted to equivalent amount of TiO_2. Simultaneous solid state detector inductively coupled plasma optical emission spectrometer (ICP-OES, model ACTIVA S, from Horiba 128 Jobin–Yvon SAS, France) was used for determination of titanium concentration. Emission

intensities were measured at two different wavelengths (308.802 nm and 334.904 nm) without separation of other elements. TiO_2 NP suspension could not be directly introduced into the nebuliser of ICP-OES, so it was digested with the help of hydrofluoric acid and nitric acid at a ratio of 1:5 in a teflon beaker and subsequently heating on a hot plate at 70-80ºC for 30 min, then evaporated to dryness by heating at 100-120 ºC. The residue was finally dissolved in 2% HNO_3 solution and made upto 25mL for analysis using ICP-OES.

2.9 Kinetic and isotherm study

Optimum quantity of Cal-Alg-SM beads was added to TiO_2 NP suspension and kept under stirring using horizontal orbital shaker at 200 rpm. The equilibrium time was evaluated by studying the amount of TiO_2 NP taken up from 100 µg mL^{-1} TiO_2 NP suspension by the sorbent beads (5 mg mL^{-1}) at different time intervals keeping pH 4.0. For the isotherm study, TiO_2 NP suspensions having different initial concentrations (1-10000 µg mL^{-1}) were exposed to fixed quantity of the sorbents (5 mg mL^{-1}) for sufficient time (24h) so that the equilibrium is established in each case.

3.0 Results and discussion

3.1 Synthesis and Characterization

Silica microspheres synthesised through sol-gel route was characterised before its impregnation into Ca-alginate matrix. The developed sorbent Cal-Alg-SM beads and the procured TiO_2 NP were also characterised.

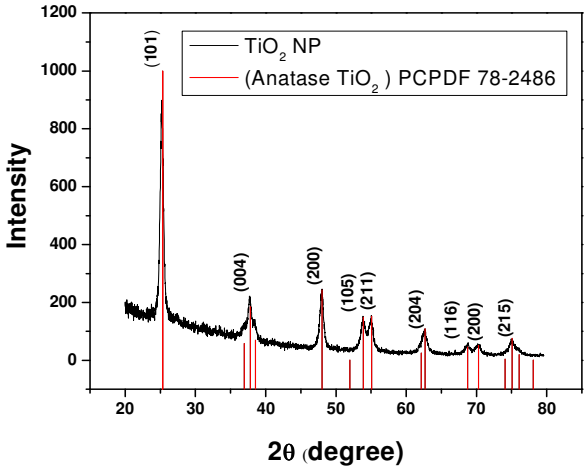

Fig. 1: XRD of TiO_2 NP (Anatase)

3.1.1 TiO_2 nano particles

The XRD analysis and Raman spectra confirms the identity of TiO_2 as anatase form.[61-62] The recorded XRD matches (Fig. 1) with the standard PCPDF card no. 78-2486 which is for the

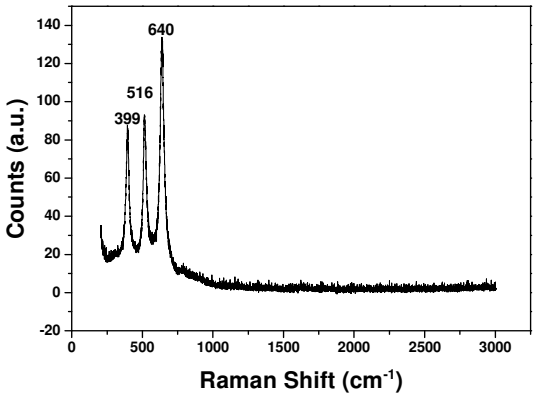

Fig. 2: Raman spectra of TiO_2 NP (Anatase)

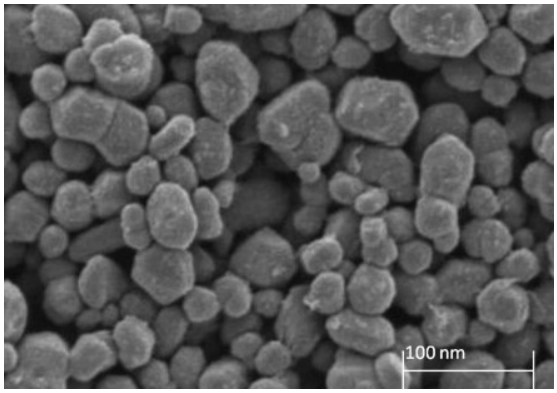

Fig. 3: SEM image of the TiO_2 NP

anatase TiO_2. Broadening of the peaks in XRD (Fig.1) suggests the smaller size of the particles, however the size was calculated using Sherrer formula considering the FWHM of the most intense peak. The size calculated was 29 nm. This was verified by measuring size by zeta sizer nano ZS which gave a mean diameter of 28.2 nm. The isoelectric point (or PZC) of TiO_2 NP was found at around pH 5 which suggests positive surface charge on the particles below pH 5 and negative surface charge above pH 5. Three major Raman shifts at 399 cm^{-1}, 516 cm^{-1} and 640 cm^{-1} (Fig. 2) also confirms the anatase phase of TiO_2 NP. SEM image as given in Fig. 3 shows the surface morphology and size of the TiO_2 NP.

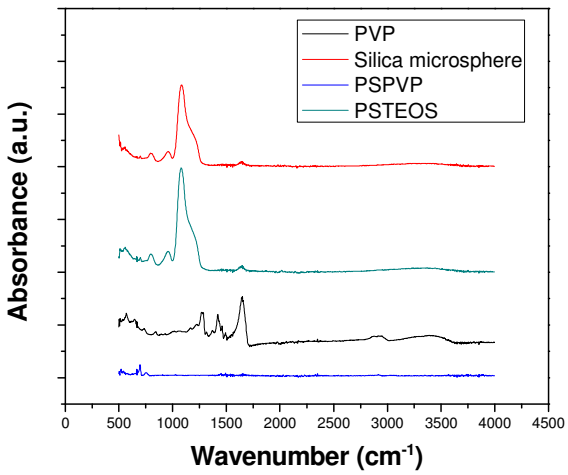

Fig. 4: ATR-FTIR at different stages of SM formation

3.1.2 Silica microspheres

In the formation of SM, PVP first participated in the polymerization reaction as a stabilizer or surfactant and then played a coupling agent role in the latter process. The polystyrene particles were dissolved subsequently or simultaneously during the sol-gel coating process followed by

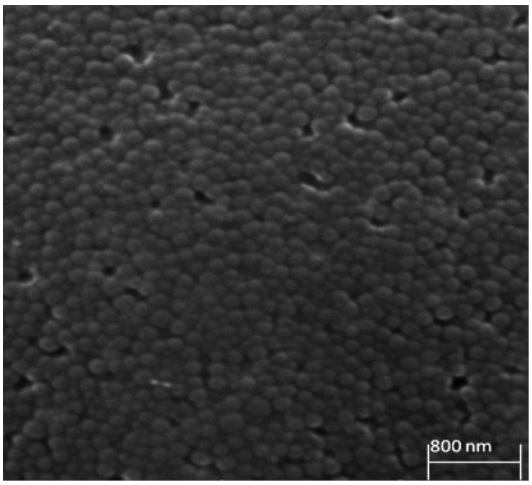

Fig. 5a: SEM image of SM

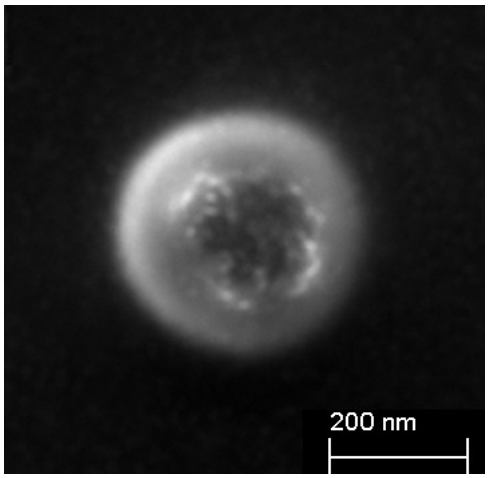

Fig. 5b: SEM image of a single SM

treatment with toluene to form silica microspheres. The size distribution of the SM as determined by the zeta sizer nano (ZS) showed mean value of 220±20 nm. The zeta potential values evaluated at various pH, showed an isoelectric point or PZC at around pH 2. The surface charge of SM originates mainly from ionization which is strongly dependent upon pH. Figure 4 shows the ATR-FTIR spectrum of the microspheres. Band at 1100 cm^{-1} in Fig.4. indicates the presence of Si-O-Si bending vibration and band at 806 cm^{-1} is due to symmetric stretching. No trace of unreacted

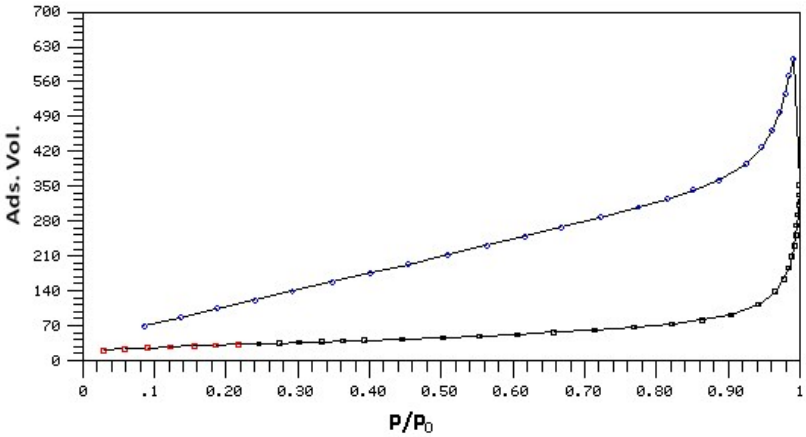

Fig. 6: BET isotherm of SM

PVP was observed in the final product which is clear from Fig.4. SEM image shows the surface morphology and spherical shape of the SM (Fig.5a and 5b). The BET measurement showed a high specific surface area (32.6 m^2 g^{-1}) of the SM making it suitable to be used as sorbent. BET isotherm for both adsorption and desorption is given in Fig. 6. Average pore diameter was found to be 1.35 nm and the pore size distribution is given in supplementary information. Detailed characterisation of SM is discussed elsewhere.[35]

3.1.3 Silica microspheres impregnated calcium alginate beads

Calcium alginate immobilization of SM involved a simple displacement reaction to form the Cal-Alg-SM beads. The uniformity of the beads in shape and size were maintained by controlling the flow rate of the homogenised mixture of SM and Na-alginate into the solution of calcium chloride by using peristaltic pump and a tube of 1.5 mm diameter. The size and shape of the beads as observed in digital image is shown in Fig.7. The average diameter of the beads was 2 ± 0.2 mm. The BET measurement showed a specific surface

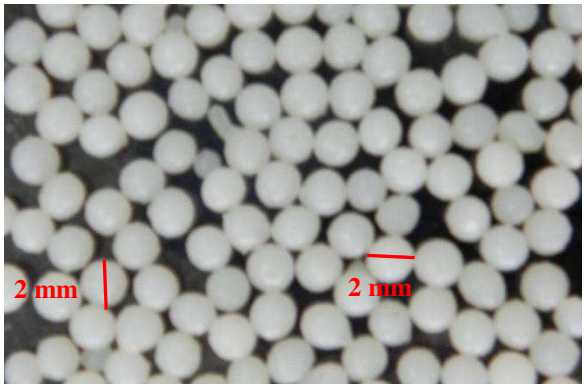

Fig. 7: Digital image of Cal-Alg-SM bead

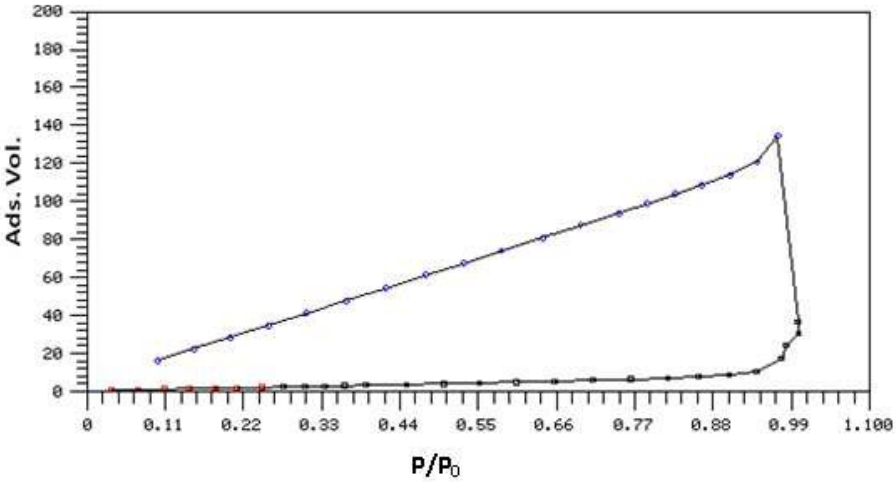

Fig. 8: BET isotherm of Cal-Alg-SM beads

area of 28.3 m^2 g^{-1} for dried Cal-Alg-SM beads. BET isotherm is given in Fig. 8. Average pore diameter was found to be 1.35 nm and the pore size distribution is given in supplementary information. The optimum composition of the beads was 10% SM loaded in 4% calcium alginate and 86% water content making it permeable to TiO_2 NP. Chemical analysis carried out after digestion of the pure beads showed that the presence of Ca, Si along with low molecular weight elements C, O, N, H which suggests proper impregnation of SM into the calcium alginate matrix. For the C, H, O, N determination elemental analysis was carried out by using Elemental analyzer [model EuroEA]. C/N , C/H ratios were obtained as 256 and 6.6 respectively.

3.2 Composition and stability of the beads

To study the effect of SM loading on calcium alginate for the sorption of TiO_2 NP, SM loading was varied from 1 to 50 wt.% and it was observed that 10% loading of SM in 4% Ca-ALG is optimum. When the loading exceeded 12%, integrity of the beads was affected and showed a tendency to be brittle.

Cal-Alg-SM beads were found to be extremely stable for months when stored in demineralised water. Stability of the beads was however checked without storing them in water. Under this condition beads were found to slowly lose the water content in it but its integrity was not affected. Beads were completely dried keeping under IR lamp and then its effectiveness for TiO_2 NP removal was checked. The uptake capacity of TiO_2 NP was not reduced when completely dried and old beads (four months) were used indicating the functional integrity of the beads.

3.3 Uptake studies

3.3.1 Uptake with different concentrations of TiO_2 NP

The sorption of TiO_2 NP on Cal-Alg-SM beads was investigated in concentration range of 10-1000 µg mL^{-1}, keeping the concentration of sorbent as 10 mg mL^{-1} in a poly-propylene container. Fig. 9 shows the variation in percentage uptake for TiO_2 NP at different initial concentrations with error bars calculated from five replicate samples. From this figure it's clear that Cal-Alg-SM beads are capable of sorbing more than 90% TiO_2 NP in concentration range of 10-500 µg mL^{-1}. Similar experiments were also been conducted to quantify the impact of Ca-alginate. It was observed that Ca-alginate could take up only 5-10% of TiO_2 NP, moreover it came out by simply washing the beads with demineralised water. In order to streamline various conditions for sorption of TiO_2 NP by Cal-Alg-SM beads, pH and time of contact were optimized.

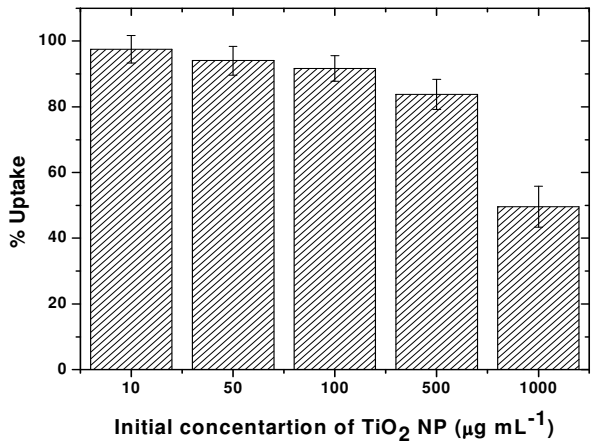

Fig. 9: Uptake of TiO_2 NP at different initial concentrations (Sorbent dose: 10 mg mL^{-1}, pH: 4-5, Time: 24h, Temperature: 25-30ºC)

3.3.2 Effect of pH

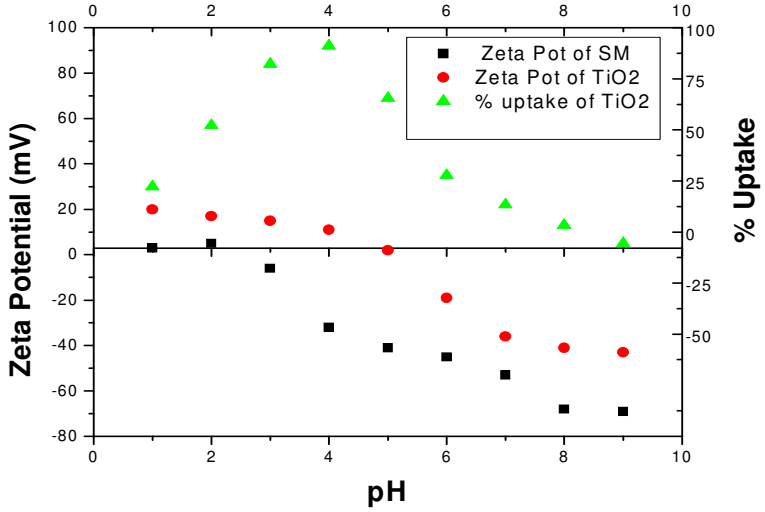

Fig. 10: % Uptake of TiO_2 NP as a function of pH and zeta potential (Initial concentrations 100 µgmL^{-1}, Sorbent dose: 5 mg mL^{-1}, Time: 24h, Temperature: 25-30ºC)

Percentage uptake of the TiO_2 NP was studied at pH range between 1-10, keeping all the sets for 24 h and having initial 100 μg mL^{-1} TiO_2 NP and sorbent as 5 mg mL^{-1}. Experimental results showed that the removal TiO_2 NP by Cal-Alg-SM beads is highly pH dependent (Fig. 10). Maximum sorption was observed at around pH 4.0. This can be explained on the basis of positive zeta potential values of TiO_2 NP below pH 5 and negative surface charge of SM above pH 2. The range of pH 3-5 is favourable for the sorption as in this window of pH the surface charges are opposite on the sorbent (SM) and sorbate (TiO_2 NP) (Fig. 6). At low pH values, both are positively charged and at high pH value also both are negatively charged and as a result sorption is not a favourable process.

3.3.3 Optimisation of contact time

In order to optimize the contact time experiments were conducted for TiO_2 NP uptake at pH 4.0 having the concentration of sorbent as 5 mg mL^{-1} for 100 μg mL^{-1} TiO_2 NP. Fig. 11 shows that sorption of TiO_2 NP increases with time up to 8 hours and then it becomes almost constant. The time for all the batch experiments was kept fixed at 8 hours henceforth to ensure maximum uptake of TiO_2 NP. The kinetics was seen to be little slow. The reason may be attributed to the slow rate of diffusion of TiO_2 NP into the alginate matrix which held the SM responsible for TiO_2 NP removal.

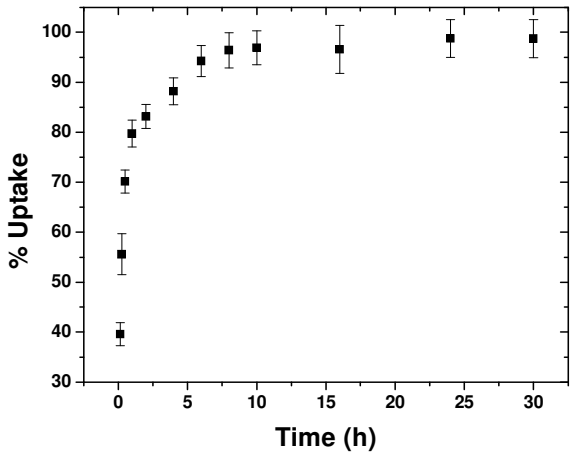

Fig. 11: Effect of contact time on the uptake of TiO_2 NP on Cal-Alg-SM beads (Initial concentration: 100 μg mL^{-1} Sorbent dose: 5 mg mL^{-1}, pH: 4, Temperature: 25-30ºC)

3.4 SEM-EDS analysis of the beads before and after the uptake

The SEM images of the beads taken before and after uptake of the TiO_2 NP (Fig. 12a & 13a) suggests that the sorbent does not possess any well-defined porous structure. EDS analysis was performed to determine the elemental constituents of pure and TiO_2 NP sorbed Cal-Alg-SM beads (Fig. 12b and 13b). In Fig. 13b spectrum shows the presence of titanium besides the principal elements Ca, Si in case of TiO_2 NP sorbed Cal-Alg-SM beads whereas no titanium peak was observed in the pure Cal-Alg-SM beads (Fig. 12b).

The mapping of titanium, scanning a specified cross-sectional area in the beads, showed no

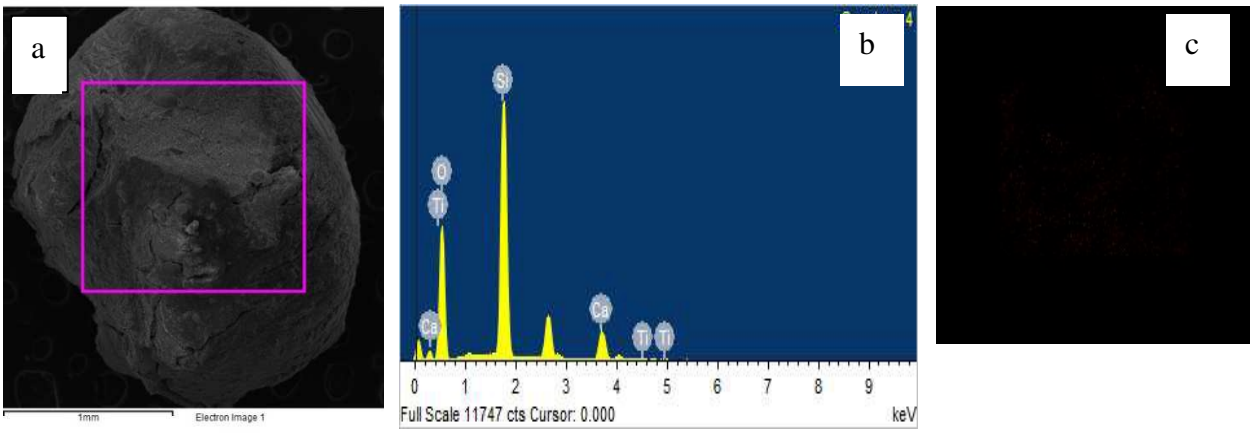

Fig. 12: SEM EDS analysis of Pure Ca-Alg-SM beads (a): SEM (b): EDS spectra (c): Elemental mapping for Ti

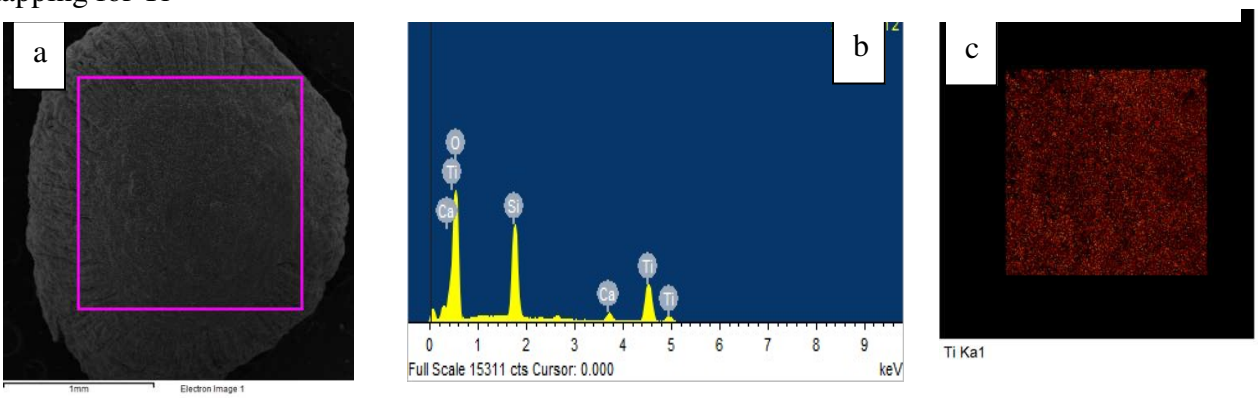

Fig. 13: SEM EDS analysis of TiO_2 NP sorbed Ca-Alg-SM beads a: SEM b: EDS spectra c: Elemental mapping for Ti

signature of Ti in case of pure beads (Fig. 12c), whereas in the case of TiO_2 NP sorbed Cal-Alg-SM beads, it was seen to be uniformly distributed (Fig. 13c).

3.5 FTIR analysis of the beads before and after the uptake

The FTIR spectra of pure and TiO_2 NP sorbed Cal-Alg-SM beads are shown in Fig.14. In FTIR spectra of Cal-Alg-SM beads taken before sorption, the peaks at 806 and 1100 cm^{-1} corresponds to the SM vibrations bands. The same peaks are not affected in case of TiO_2 NP sorbed Ca-Alg-SM beads. These observations suggest that probably no direct bonding takes place between Cal-Alg-SM beads and TiO_2 NP, therefore the interaction may be due to electrostatic attraction or due to adsorption.

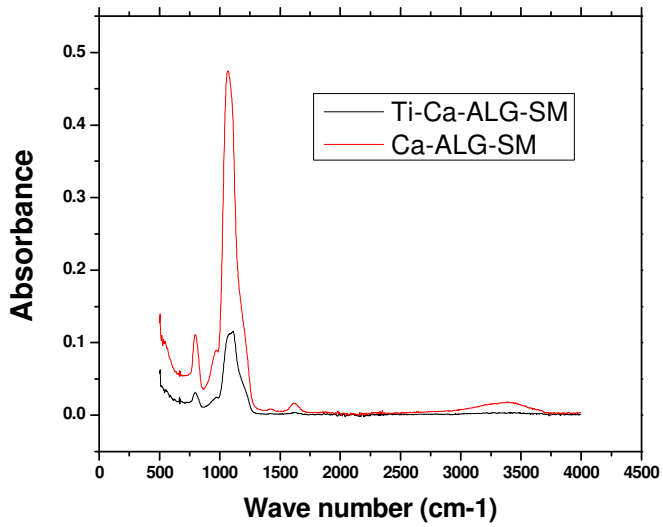

Fig: 14: ATR-FTIR spectra of pure and TiO_2 NP sorbed Ca-Alg-SM beads

3.6 Sorption isotherm

In order to evaluate the sorption capacity of Cal-Alg-SM beads for TiO_2 NP, the equilibrium sorption of TiO_2 NP was studied as a function of TiO_2 NP concentration at 25-30 ^{O}C. The sorption isotherms are given for Langmuir (Equation 2) and Freundlich (Equation 3) isotherms respectively.

$$Q_e = Q_o b C_e/(1 + bC_e) \quad (2)$$

$$Q_e = kC_e^{1/n} \quad (3)$$

where Qe is the amount of sorbate per unit mass of sorbent (mg g^{-1}) at equilibrium, Ce is the equilibrium concentration of sorbent. The Langmuir isotherm as given in equation 2 assumes that

the free energy of adsorption does not depend on the surface coverage. It also predicts the solid surface saturation with monolayer coverage of adsorbate at high C_e and a linear adsorption at low C_e values. Q_0 is the solid phase concentration corresponding to the complete monolayer coverage of adsorption sites and b is a constant related to the free energy of adsorption.[63]

Freundlich isotherm model (equation 3) assumes that the ratio of the amount of solute sorbed onto a given mass of sorbent to the concentration of the solute in the solutions is not constant at different solution concentrations. The constants n and k in the Freundlich model are related to the strength of the adsorptive bond and the bond distribution.[63]

It is clear from the isotherm plots that Langmuir isotherm (Fig. 15) fits the experimental data well with the R^2 value of 0.99 in comparison to the Freundlich model (R^2 = 0.96) (Fig. 16).

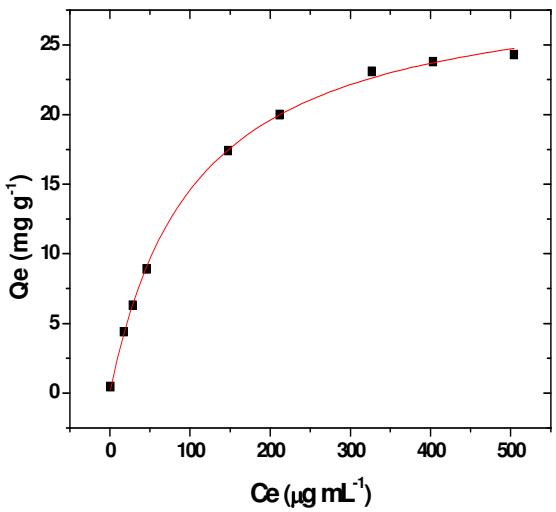

Fig: 15: Langmuir isotherm plot for TiO_2 NP sorption on Ca-Alg-SM beads (Sorbent dose: 5 mg mL^{-1}, pH: 4, Time: 8h, Temperature: 25-30ºC).

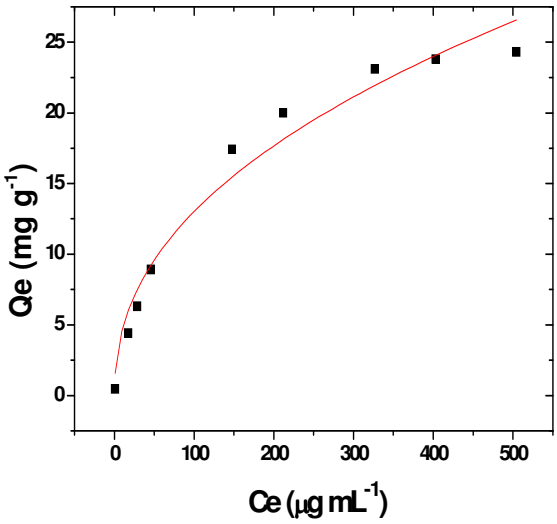

Fig: 16: Freundlich isotherm plot for TiO_2 NP sorption on Ca-Alg-SM beads (Sorbent dose: 5 mg mL^{-1}, pH: 4, Time: 8h, Temperature: 25-30ºC).

This indicates that the sorption of TiO_2 NP on Cal-Alg-SM beads is a monolayer adsorption. The monolayer adsorption capacity which is measured as the Langmuir constant Q_0, was obtained as

29.9 mg g^{-1} from fitting (Fig. 15) and it is very close to the experimentally determined sorption capacity (28.4 mg g^{-1}).

3.7 Sorption kinetic modelling of TiO_2 NP on Cal-Alg-SM beads

To study the dynamics of the solute adsorption process, the kinetics of TiO_2 NP sorption on Cal-Alg-SM beads was analyzed using pseudo-first-order (Equation 4) and pseudo-second-order kinetic models (Equation 5) keeping other parameters constant[64-65] (Concentration of TiO_2 NP 100 µg mL^{-1}, pH 4, dose rate 5 mg mL^{-1}).

$$\log(q_e - q_t) = \log q_e - K_1/2.303\ t \quad (4)$$

$$t/q_t = 1/K_2 q_e^2 + (1/q_e)t \quad (5)$$

where q_e is the amount of TiO_2 NP sorbed on Cal-Alg-SM (mgg^{-1}) at equilibrium; q_t is the amount of TiO_2 NP sorbed on Cal-Alg-SM (mg g^{-1}) at time t (h); k_1 is the rate constant for the pseudo-first-order kinetics and k_2 is the rate constant for the pseudo-second order kinetics.

From the linear correlation coefficient (R^2) values it was clear that the pseudo-second-order rate law was fitted well (R^2=0.99) as given in Figure 17 compared to the pseudo-first-order model (R^2=0.75). The rate constant value was obtained as 0.165 g $mg^{-1}h^{-1}$ using the slope (for q_e) and intercept of the fitted line.

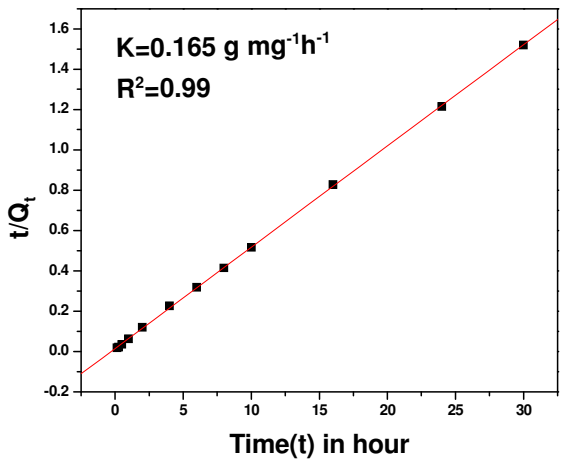

Fig. 17: Pseudo-second-order kinetic fitting of TiO_2 NP sorption on Cal-Alg-SM beads (Concentration of TiO_2 NP 100 µg mL^{-1}, pH 4, dose rate 5 mg mL^{-1}, Temperature: 25-30ºC).

3.8 Monitoring of drinking water quality after treatment with the Ca-Alg-SM beads and effectiveness for real water samples

Table 1: Physicochemical characteristics of lake and groundwater before and after removal of TiO_2 NP using Cal-Alg-SM beads.

Parameters	Before treatment	After treatment
pH	5.5-7.6	5.7-7.7
Conductance (μ S)	321-406	346-398
Redox potential (mV)	118-125	121-129
DOC (mg L^{-1})	8-10	9-12
Cl^{-1} (mg L^{-1})	17.5-20.6	18.1 -20.9
PO_4^{3-} (mg L^{-1})	0.52-0.57	0.52-0.57
Na(mg L^{-1})	23.2-28.2	23.4-28.7
K (mg L^{-1})	0.85-0.90	0.78-0.89
Mg (mg L^{-1})	14.4-15.9	15.3-16.4
Ca (mg L^{-1})	40.1-43.7	39.8-43.9
Cu (μg L^{-1})	5.5-8.6	5.3-7.9
Fe (mg L^{-1})	1.5-2.1	1.6-2.1
Si (mg L^{-1})	38.3-51.6	39.1-51.7
Experimental conditions: Sorbent dose: 5 mg mL^{-1}, Time: 8h, Initial TiO_2 NP concentration: 10 μg mL^{-1}, Temperature: 25-30ºC.		

Table-1 shows various physicochemical characteristics of lake and groundwater samples used for this study, both before and after the treatment with the Cal-Alg-SM beads for removal of TiO_2 NP. They were used for spiking with TiO_2 NP. It was clear from Table-1, which gives the range of the physicochemical parameters, that no major variation of any particular property was observed due to the treatment with the beads. No elevated level of concentration after the treatment, assures the drinkability of the water. Special care was taken for calcium (Ca), silica (Si) and alginate which are the components of the beads. Results showed no elevated level of

Table 2: Decrease in concentration of TiO_2 NP after the treatment in four different samples

Sample identification	Spiked concentration of TiO_2 NP (ng mL^{-1})	Concentration of TiO_2 NP after treatment with the beads (ng mL^{-1})
Groundwater -1	1000	32
Groundwater -2	1000	17
Groundwater-3	1000	26
Lake water	1000	Below detection limit (<10)
Experimental conditions: Sorbent dose: 5 mg mL^{-1}, Time: 8h, pH:4-5, Temperature: 25-30ºC.		

concentrations of Ca, Si and DOC (dissolved organic content) in the water after treatment, suggesting no leaching of any of the components from the beads.

Real water samples were spiked with TiO_2 NP and the beads were successfully tested to decontaminate. Table 2 gives the concentrations of TiO_2 NP before and after treatment with Cal-Alg-SM beads.

3.9 Mechanism of sorption

Mechanism of the uptake is governed by the sorption of TiO_2 NP species on silica microspheres. The surface chemistry of both SM and TiO_2 NP varies with pH. It is clear from Fig. 6 that the PZC of SM is about pH 2 and for TiO_2 NP is around pH 5. At these pH, the hydroxyl group of both SM and TiO_2 NP is protonated with only one proton and net surface charge becomes zero. At low pH value, the hydroxyl groups at the surface of the SM (SiO_2) are doubly protonated and thus the surface charge of the SM is positive. But at pH above 2.0; SM is negatively charged which is clear from the zeta potential values. Similarly TiO_2 NP is having positive surface charge below pH 5.0.

Maximum sorption of TiO_2 NP was observed at pH around 3-5 according to our experimental result. At this pH range, the electrostatic attraction between the negative oxoanion of SM and the positive surface charge on TiO_2 NP favours sorption. At lower pH value (pH<2), fully protonated species of both TiO_2 NP and SM are present in solution therefore electrostatic attraction is no longer possible which results in a lower sorption. At pH above 5, both are negatively charged and repel each other and consequently sorption decreases. The sorption of TiO_2 NP having positive surface charge is enhanced by the presence of carboxylic acid and hydroxyl groups in the alginate. But the most important role the alginate serves, is to bind the

SM into the matrix and because of the formation of the beads separation of the sorbent becomes easy.

3.10 Recovery of TiO_2 NP from Cal-Alg-SM beads

Recovery of the sorbate (TiO_2 NP) from the saturated Cal-Alg-SM beads, was carried out with two different eluents (a) 0.5 M HNO_3 and (b) mixture of 0.5 M HNO_3 and 1% solution of 30% HF. It was observed that the recoveries were in the range of 5-10% only. Therefore, total recovery of TiO_2 NP from Cal-Alg-SM was carried out by complete destruction of beads using HNO_3 (16N) and HF (30%) in the ratio of 3:1. More than 99% recovery of the sorbate was achieved.

4.0 Conclusion

The results from the current study exhibit the potential of Cal-Alg-SM beads for TiO_2 nanoparticles removal from potable water at pH 3-5 without disturbing the water qualities. Various parameters for synthesis of the stable beads were optimised. The sorption capacity of the beads for TiO_2 nanoparticles was evaluated as 29.9 mg g^{-1} at 25–35° C from Langmuir isotherm model and this matched well with the experimentally determined value. The kinetics followed pseudo second order rate law. The Fourier Transform Infra Red spectra and Scanning Electron Microscope hyphenated with Energy dispersive spectrometer analysis provided an understanding of the interaction between TiO_2 NP and silica microspheres impregnated into Ca-Alginate. Mechanism of sorption could be proposed based on the zeta potential values of both silica microspheres and TiO_2 nanoparticles at different pH.

Acknowledgments

The authors sincerely acknowledge the encouragement and guidance provided by Dr. B.N.Jagatap, Director, Chemistry Group.

References

1. E. R. Kisin, A. R. Murray, M. J. Keane, X. C. Shi, D. Schwegler-Berry, O. Gorelik, S. Arepalli, V. Castranova, W. E. Wallace, V. E. Kagan and A. A. Shvedova, *J. Toxicol. Environ. Health A*, 2007, **70**, 2071–2079.
2. T. A. Robertson, W. Y. Sanchez and M. S. Roberts, *J. Biomed. Nanotechnol.*, 2010, **6**, 452–468.
3. H. Shi, R. Magaye, V. Castranova and J. Zhao, *Part. Fibre. Toxicol.,* 2013, **10**:15.
4. S. M. Gupta and M. Tripathi, *Chin. Sci. Bull*, 2011, **56**, 1639–1657.
5. J. Riu, A. Maroto and F. X. Rius, *Talanta*, 2006, **69**, 288–301.
6. M. J. Z. Ruth, B. Linda and D. Min, *Exp. Ther. Med.*, 2012, **4**, 551–561.
7. P. Z. Ray and H. J. Shipley, *RSC Adv*., 2015, **5**, 29885- 29907.
8. I. Ali, *Chem. Rev*., 2012, **112**, 5073−5091.
9. Threshold limit values and biological exposure indices for 1992–1993. Cincinnati: Ohio: American Conference of Governmental industrial hygienists; 1992.
10. Participants IRSIW: A workshop consensus report, *Inhal Toxicol*, 2000, **12**, 1–17.
11. M. Ortlieb, *GIT Lab. J. Eur.,* 2010, **14**, 42–43.
12. R. K. Shukla, V. Sharma, A. K. Pandey, S. Singh, S. Sultana and A. Dhawan, *Toxicol. In Vitro*, 2011, **25**, 231–241.
13. J. J. Wang, B. J. Sanderson and H. Wang, *Mutat. Res*., 2007, **628**, 99–106.
14. R. Baan, K. Straif, Y. Grosse, B. Secretan, F. Ghissassi El and V. Cogliano, *Lancet. Oncol.,* 2006, **7**, 295–296.
15. T. Kaida, K. Kobayashi, M. Adachi and F. Suzuki, *J. Cosmet. Sci.*, 2004, **55**, 219–220.

16. R. Wolf, H. Matz, E. Orion and J. Lipozencic, *Acta Dermatovenerol Croat*, 2003, **11**, 158–162.

17. A. D. Maynard and E. D. Kuempel, *J. Nanopart. Res*., 2005, **6**, 587–614.

18. J. S. Tsuji, A. D. Maynard, P. C. Howard, J. T. James, C. W. Lam, D. B. Warheit and A. B. Santamaria, *Toxicol. Sci.,* 2006, **89**, 42–50.

19. J. Zhao, L. Bowman, X. Zhang, V. Vallyathan, S. H. Young, V. Castranova and M. Ding, *J. Toxicol. Environ. Health A*, 2009, **72**, 1141–1149.

20. K. P. Lee, H. J. Trochimowicz and C. F. Reinhardt, *Toxicol. Appl. Pharmacol.*, 1985, **79**, 179–192.

21. E. Fabian, R. Landsiedel, L. Ma-Hock, K. Wiench, W. Wohlleben and B. van Ravenzwaay, *Arch. Toxicol.*, 2008, **82**, 151–157.

22. G. Oberdorster, *Int. Arch. Occup. Environ. Health*, 2001, **74**, 1–8.

23. G. Oberdorster, J. Ferin and B. E. Lehnert, *Environ. Health Perspect*, 1994, **102** (Suppl 5), 173–179.

24. T. M. Sager, C. Kommineni and V. Castranova, *Part Fibre. Toxicol.*, 2008, **5**, 17.

25. IARC, Sci Publ, 2006, **86**.

26. T. C. Long, J. Tajuba, P. Sama, N. Saleh, C. Swartz, J. Parker, S. Hester, G. V. Lowry and B. Veronesi, *Environ. Health Perspect.*, 2007, **115**, 1631–1637.

27. I. Ali, *Sepn. Purfn. Rev.*, 2010, **39**, 95–171.

28. I. Ali, *Sepn. Purfn. Rev.*, 2014, **43**, 175–2015.

29. I. Ali, M. Asim and T. A. Khan, *Journal of Environ Management,* 2012, **113**, 170-183.

30. V. K. Gupta and I. Ali, *Nature Protocols*, 2006, **1**, 2661–2667.

31. R. K. Singhal, H. Basu and A. V. R. Reddy, *J. Environ. Anal. Chem.*, 2014, 1:2.

32. L. Guangyu, H. Zhang, X. Yang and Y. Wang, *Polymer,* 2007, **48**, 5896–5904.

33. M. Emadi, E. Shams and M. K. Amini, , *Journal of Chemistry*, Article ID **787682,** 2013.

34. J. Qu, W. Li, C. Y. Cao, X. J. Yin, Liang Zhao, J. Bai, Z. Qinc and W. G. Song, *J. Mater. Chem.*, 2012, **22**, 17222-17226.

35. H. Basu, R. K. Singhal, M. V. Pimple and A. V. R. Reddy, *Int. J. Environ. Sci. Tech.*, 2015, **12**, 1899-1906.

36. H. Basu, R. K. Singhal, M. V. Pimple, Manisha V., M. K. T. Bassan, A. V. R. Reddy and T. Mukherjee, *J. Radioanal. Nucl. Chem.*, 2011, **289**, 231–237.

37. H. Li, W. Li, Y. Zhang, T. Wang, B. Wang, W. Xu, L. Jiang, W. Song, C. Shu and C. Wang, *J. Mater. Chem.*, 2011, **21**, 7878-7881.

38. H. Basu, R.K. Singhal, M. V. Pimple, A. Kumar and A. V. R. Reddy, *J. Radioanal. Nucl. Chem.*, 2014, **303**, 2283–2291.

39. L. L. Hench and J. K. West, *Chem. Rev.,* 1990, **90**, 33–72.

40. C. Frank, R. A. Caruso and H. Mohwald, *Science*, 1998, **282**, 1111–1118.

41. T. Zhang, J. Ge, Y. Hu, Q. Zhang, S. Aloni and Y. Yin, *Angew Chem.*, 2008, **120**, 5890–5895.

42. H. Zou, S. Wu, Q. Ran and J. Shen, *J. Phys. Chem. C*, 2008, **112**, 11623–11629.

43. W. Li, C. Y. Cao, L. Y. Wu, M. F. Ge and W. G. Song, *J. Hazard. Mater.*, 2011, **198**, 143-150.

44. R. Naseem and S. S. Tahir, Water Res. 2001, **35**, 3982–3986.

45. C. Rosaria, M. Sciortino, G. Alonzo, A. D. Schrijver and M. Pagliaro, *Chem. Rev., 2011,* **111**, 765–789.

46. W. Li , F. Xia, J. Qu, P. Li , D. Chen , Z. Chen , Y. Yu , Y. Lu , R. A. Caruso and W. Song, *Nano Res.*, 2014, **7**, 903-916.

47. W. Li, D. Chen, F. Xia, J. Z. Y. Tan, P. P. Huang, W. G. Song, N. M. Nursam and R. A. Caruso, *Environ. Sci.: Nano,* 2016, Advance Article, DOI: 10.1039/C5EN00171D.

48. Y. Wang, G. Wang, H. Wang, C. Liang, W. Cai and L. Zhang, *Chem Eur J*., 2010, **16**, 3497–3503.

49. Y. Zhuang, Y. Yang, G. Xiang and X. Wang, *J. Phys. Chem. C*, 2009, **113**, 10441–10445.

50. P. K. Jal, S. Patel and B. K. Mishra, *Talanta*, 2004, **62**, 1005–1028.

51. R. K. Singhal, H. Basu, and A. V. R. Reddy, *J. Radioanal. Nucl. Chem.*, 2013, **295**, 1345-1351.

52. H. Mimura, H. Ohta, H. Hoshi, K. Akiba, Y. Wakui and Y. Onodera, *J. Radioanal. Nucl. Chem.,* 2001, **247**, 33–38.

53. R. K. Singhal, H. Basu, Manisha V., A. V. R. Reddy and T. Mukherjee, *Desalination*, 2011, **280**, 313–318.

54. M. Outokesh, H. Mimura, Y. Niibori and K. Tanaka, *J. Microencapsulation*, 2006, **17**, 291–301.

55. R. K. Singhal, S. Joshi, K. Tirumalesh and R. P. Gurg, *J. Radioanal. Nucl. Chem.*, 2004, **261**, 73–78.

56. H. Mimura, H. Ohta, H. Hoshi, K. Akiba, Y. Wakui and Y. Onodera, *J. Nucl. Sci. Technol.*, 2002, **39**, 283–285.

57. H. Basu, R. K. Singhal, M. V. Pimple and A. V. R. Reddy, *Water Air Soil poll., 2013,* **224**:1572.

58. B. Achintya, N. Krajangpan, S. Chisholmb, J. Bret, E. Khan, J. Bermudez and J. Elorza, *J. Hazard. Mater.*, 2009, **166**, 1339–1343.

59. H. Basu, R. K. Singhal, M. V. Pimple and A. V. R. Reddy, *Water Air Soil poll., 2015,* **226**: 22.

60. A. Banerjee and D. Nayak, *Bioresour. Technol.*, 2007, **98**, 2771–2774.

61. L. Cao, D. Chen, W. Li and R. A. Caruso, *ACS Appl. Mater. Interfaces*, 2014, **6,** 13129–13137.

62. Y. Yu, C. Cao , W. Li , P. Li, J. Qu and W. Song, *Nano Res.,* 2012, **5**, 434-442.

63. V. K. Gupta, S. Sharma, I. S. Yadav and M. Dinesh, *J. Chem. Technol. Biotechnol.*, 1998, **71**, 180–186.

64. M. C. Kimling, N. Scales, T. L. Hanley and R. A. Caruso, *Environ. Sci. Technol.*, 2012, **46**, 7913–7920.

65. Y. S. Ho and G. McKay, *Process Biochem.*, 1999, **34**, 451–465.

Graphical Abstract

Development of new hybrid material (Cal-Alg-SM beads) for TiO_2 nanoparticle uptake without disturbing the water quality parameters.

Cal-Alg-SM beads